International Journal of Nanomedicine

Dovepress
open access to scientific and medical research

Open Access Full Text Article

ORIGINAL RESEARCH

Co-Delivery of Docetaxel and Curcumin via Nanomicelles for Enhancing Anti-Ovarian Cancer Treatment

This article was published in the following Dove Press journal:
International Journal of Nanomedicine

Yuzhu Hu[1,2]
Mengni Ran[1]
Bilan Wang[3]
Yunzhu Lin[3]
Yongzhong Cheng[1]
Songping Zheng[1]

[1]Department of Neurosurgery and Institute of Neurosurgery, State Key Laboratory of Biotherapy, West China Hospital, West China Medical School, Sichuan University and Collaborative Innovation Center for Biotherapy, Chengdu 610041, People's Republic of China; [2]Department of Medical Oncology, Cancer Center, West China Hospital, West China Medical School, Sichuan University, Chengdu 610041, People's Republic of China; [3]Department of Pharmacy, West China Second University Hospital, Sichuan University, Chengdu 610041, People's Republic of China

Introductions: Ovarian cancer is a stubborn malignancy of gynecological system with a high mortality rate. Docetaxel (DTX), the second-generation of anti-tumor drug Taxane, has shown superior efficacy over classic paclitaxel (PTX) in certain cancers. However, its clinical application is hindered by poor bioavailability. The natural spice extract curcumin (Cur) has been discovered to improve the bioavailability of DTX. Therefore, it is meaningful to develop a combined drug strategy of DTX and Cur with methoxy poly (ethylene glycol)-poly (L-lactic acid) (MPEG-PLA) copolymers in ovarian cancer therapy.

Methods: Injectable DTX-Cur/M nanomicelles were synthesized and characterized in the study. The molecular interactions between DTX, Cur and copolymer were simulated and the drug release behavior was investigated. The anti-tumor activity and anti-tumor mechanisms of DTX-Cur/M were evaluated and explored in both cells and mice model of xenograft human ovarian cancer.

Results: DTX-Cur/M nanomicelles with an average particle size of 37.63 nm were obtained. The drug release experiment showed sustained drug release from DTX-Cur/M nanomicelles. The MTT assay and apoptotic study indicated that DTX-Cur/M exhibited stronger inhibition and pro-apoptotic effects on A2780 cells compared with DTX or Cur alone. In vivo anti-tumor experiment results confirmed that the DTX-Cur/M played the most effective role in anti-ovarian cancer therapy by inhibiting tumor proliferation, suppressing tumor angiogenesis and promoting tumor apoptosis.

Conclusion: We designed injectable DTX-Cur/M nanomicelles for co-delivery of DTX and Cur agents to the tumor site through systemic administration. The DTX-Cur/M nanomicelle would be a biodegradable, sustainable and powerful anti-tumor drug candidate with great potential in ovarian cancer treatment.

Keywords: docetaxel, curcumin, ovarian cancer, nanocarrier, co-delivery

Introduction

Ovarian cancer is a gynecological malignant tumor with high morbidity and mortality. There is a lack of effective screening approach for ovarian cancer at present. A majority of patients were diagnosed with advanced stage ovarian cancer and exhibited high recurrence rate of 60–80%.[1–3] The standard treatment for ovarian cancer is surgery and platinum and taxane-based chemotherapy.[4–6] Several targeted drugs, including anti-angiogenesis agent Bevacizumab and poly (adenosine diphosphate-ribose) polymerase PARP inhibitors such as Olaparib, have recently been applied in the maintenance therapy for ovarian cancer.[7,8] Despite global effort to improve the prognosis of ovarian

Correspondence: Yongzhong Cheng; Songping Zheng
Tel +86 28 8516 4063
Email chengyz@scu.edu.cn; 13618088051@163.com

submit your manuscript | www.dovepress.com
DovePress
http://doi.org/10.2147/IJN.S274083

cancer, the five-year survival rate of patients with stage III and stage V (FIGO) ovarian cancer are only about 39% and 17%, respectively.[9] There is an urgent need to develop more powerful drugs to make significant progress in the management of ovarian cancer.

Taxane cytotoxic drugs represented by paclitaxel (PTX) and docetaxel (DTX) have become one of the most effective therapeutic agents in gynecological cancer in recent decades. DTX is a second-generation Taxane drug, which functions through inhibiting cancer cells' mitosis and proliferation by promoting tubulin polymerization and preventing tubulin depolymerization.[10] DTX exhibited higher solubility and better bioavailability than PTX.[11,12] Its clinical efficacy against many malignant cancers is superior to PTX, attributed to three times higher intracellular concentration, longer retention time and 100-fold greater phosphorylation of Bcl-2 than PTX.[13,14] DTX has been approved for the treatment of prostate cancer, breast cancer, lung cancer, ovarian cancer, head and neck cancer and gastric cancer.[15–22] However, poor water solubility, non-selective distribution and drug resistance hinder the clinical application of DTX. Researchers are keen to overcome these obstacles and improve the therapeutic efficacy of DTX.

Drug combination therapy is very efficient and promising in cancer treatment.[23–25] Curcumin (Cur) is a natural product derived from Asian spice *Curcumin longa*, which has shown beneficial effects in the treatment of various diseases.[26,27] Due to its low toxicity and anti-tumor capability, Cur has attracted much attention as a cancer therapeutic agent.[28–30] Intriguingly, the bioavailability of DTX is mainly affected by cytochrome P450 (CYP3A) and membrane transporter P-glycoprotein (P-gp),[31,32] while Cur could suppress the expression and the activity of CYP3A enzyme and P-gp.[33] The pre-treatment of Cur in rats before oral administration of DTX proved to enhance the bioavailability of DTX.[34] Thereupon, it is appealing to develop combined delivery strategy of DTX and Cur, and explore its anti-tumor effect in ovarian cancer therapy. Both DTX and Cur have the drawback of poor water solubility.[35] With the aim to improve drug bioavailability, we prepared biodegradable methoxy poly (ethylene glycol)-poly (L-lactic acid) MPEG-PLA nanomicelles loaded with DTX and Cur for intravenous injection in the study. The water-insoluble drug agents were successfully encapsulated into the amphiphilic micelle composed with MPEG-PLA co-polymers, which could suspend under aqueous condition and become injectable. The characteristics, molecular dynamics, release behavior and both in vitro and in vivo anti-tumor activities of DTX-Cur/M nanomicelles were investigated in this study. Finally, we hope this research will provide a new insight for the treatment of ovarian cancer.

Materials and Methods

Materials

MPEG, anhydrous L-lactic acid, Cur and 3-(4, 5-dimethylthiazol-2-yl)-2, 5-diphenyltetrazolium bromide (MTT) were purchased from Sigma Aldrich (USA). DTX was purchased from Sichuan Xieli Pharmaceutical (China). Dulbecco's Modified Eagle's Medium (DMEM) and fetal bovine serum (FBS) were purchased from Gibco BRL (USA). Dimethyl sulfoxide (DMSO) and acetone were purchased from KeLong Chemicals (China). All primary and horseradish peroxidase (HRP) conjugated antibodies were purchased from Servicebio (China). Other chemicals used in the study were analytical grade and obtained commercially. Human A2780 ovarian carcinoma cells were purchased from American Type Culture Collection (ATCC, USA). 7–8 weeks female BALB/c athymic nude mice (HFK Bioscience, Beijing, China) were obtained and fed with sterilized water and chow. All animal procedures were performed following the protocol approved by the Institutional Animal Care and Treatment Committee of Sichuan University and conducted according to the Institutional Animal Care and Use Guidelines.

Preparation and Characterization of DTX-Cur/M

The DTX-Cur/M nanomicelle was prepared at two steps. Firstly, the synthesis procedure of MPEG-PLA copolymers was according to our previous report.[36] The obtained product was lyophilized and stored in a desiccator. Then, DTX (5 mg), Cur (5 mg) and MPEG-PLA copolymers (90 mg) were dissolved in 2 mL acetone. The mixture was evaporated with constant stirring under reduced pressure in 55°C water bath to form a thin film. Consequently, normal saline was added into the mixture to form self-assembly nanomicelles. The DTX, Cur, and co-polymers spontaneously assembled to form a core–shell structure that wrapped Cur and DTX inside the hydrophobic core. Moreover, the un-encapsulated drug was removed by filtering with a 0.22 μm membrane (Millipore, USA). The empty micelles, Cur/M micelles and DTX/M micelles were prepared accordingly.

Dynamic light scattering (DLS) method was employed to detect the average particle size and zeta-potential of the obtained DTX-Cur/M (Malvern Nano-ZS 90, UK). After negatively stained by phosphotungstic acid for 10 min and dried in air, the particle size and morphology of DTX-Cur /M was observed by transmission electron microscopy (TEM) (Hitachi, Japan). In addition, 10 mg of DTX-Cur /M dissolved in 0.1 mL acetonitrile was analyzed by high performance liquid chromatography (HPLC) (Shimadzu, Japan). The entrapment efficiency (EE) and drug loading (DL) were calculated according to the following equations: EE=100%×experimental drug loading/theoretical drug loading; DL=100%×drug/(drug + polymer).

Interactions Between DTX, Cur and MPEG-PLA Polymers

DTX and Cur were initially built with Marvin Sketch (http://www.chemaxon.com) and then optimized using MMFF994 method.[37] The semi-empirical approach AM1 was further employed to optimize the molecular structures with Fletcher-Reeves algorithm.[38] This process was accomplished by HyperChem software (USA). The structures of MPEG-PLA was constructed, optimized and simulated referring to the published literature.[39] The interactions between DTX, Cur and MPEG-PLA copolymers were explored in the study. Briefly, DTX and Cur were firstly randomly docked to the simulated MPEG-PLA in the workspace of HyperChem, thus to obtain the original structure of DTX-Cur/M complex. Then, the Langevin's dynamics simulation was performed to explore the interaction between the three components in water environment. The temperature, friction coefficient and random seed were set as 300K, 0.05 ps^{-1} and 0, respectively. The force field used was CHARMM27. The interaction in water was simulated at the first stage. In consideration of the solvation effect, the scale factor for dielectric permittivity was set as 80. The run time for each stage was 500 picoseconds.

Drug Release Study

In vitro release behavior of DTX-Cur/M was investigated with the dialysis method. During the experiment, 1 mL of DTX-Cur/M containing 2 mg DTX and 2 mg Cur was placed in a dialysis bag and incubated in 20 mL of PBS (pH 7.4) containing 0.5% (v/v) Tween-80 (PBST) under gentle shaking. During the process, the medium was replaced with fresh medium at different intervals (0, 2, 6, 12, 24, 36, 48, 72, 96 and 120 h). The amount of DTX or Cur in the incubation medium was quantified by determining the absorbance at 230 nm or 421 nm using HPLC, respectively. This study was repeated three times.

In vitro Cellular Experiments

A2780 cells were cultured in DMEM culture medium containing 10% FBS, 100 U/mL penicillin and 100 μg/mL streptomycin. The cells were incubated in a humid environment at 37°C with 5% CO_2. Cells at logarithmic phase were seeded in a 96-well plate at the density of 3.5×10^3 cells per well. After overnight incubation, different concentrations of Cur/M, DTX/M or DTX-Cur/M were added and treated cells for 24 hrs or 48 hrs. The culture medium was then replaced by fresh medium containing MTT (5 mg/mL) to form formazan, which would be dissolved in DMSO and presented in purple color. The optical density of each well at 570 nm was determined by a microplate reader (OPTImax, USA). The relative cell viability was calculated by dividing the optical density of treated cells with the optical density of control cells. The experiment was replicated three times.

Propidium Iodide (PI)/Annexin-V apoptosis detection kit (BD, USA) was used to investigate tumor cells apoptosis after different treatments. The cells treated with different concentrations of Cur-M, DTX-M and DTX-Cur/M for 48 hrs were harvested and washed by PBS twice. Subsequently, 100 μL binding buffer containing 3 μL PI and 3 μL Annexin-V was added to suspend and stain cells in each tube. After 0.5 hr, another 300 μL binding buffer was added and the stained cells were analyzed by a flow cytometer (ACEA, Novocyte, USA).

In vivo Anti-Tumor Therapy

With the aim to evaluate the anti-tumor ability in vivo, a nude mice model of human ovarian cancer was established in the study by implanting 1×10^7 A2780 cells in the right flank of mice. The therapy started on the 7th day after tumor inoculation, when the average size of subcutaneous tumor reached $100mm^3$. All experimental mice were randomly allocated into five groups and received the following treatment: Control: solvent, M: MPEG-PLA nanomicelles, Cur/M: 8 mg/kg Cur, DTX/M: 8 mg/kg DTX, DTX-Cur/M: 8 mg/kg (1:1). Individual treatment was given by tail vein injection every four days. Tumor volume and mice body weight was monitored and recorded during the experiment. The mice were sacrificed 31 days after tumor inoculation and the tumors were collected for further analysis.

Immunohistochemical Study

The immunohistochemical staining of Ki67 and CD31 were carried out according to the procedures described previously.[40] Briefly, the tumor sections were sequentially stained with primary antibody of Ki67 or CD31 and secondary HRP-conjugated antibody, followed by DAB coloration and hematoxylin counterstain. The stained tumor sections were observed under light microscope and evaluated for tumor proliferation and tumor angiogenesis. Five random fields at 400× magnification were selected for quantitative analysis. The Ki67 index was defined as the number of Ki67 positive divided by the number of whole cells. Micro-vessel density (MVD) was defined as the number of CD31 positive cells in the high-power field.

TUNEL Assay

The DNA fragmentation in apoptotic cells of tumor were determined by the terminal deoxynucleotidyl transferase (TdT)-mediated dUTP Nick-End Labeling (TUNEL) apoptosis detection kit (Promega, USA). All procedures were conducted according to the manufacture description. The stained sections were observed under fluorescence microscopy and evaluated for tumor apoptosis. Five random fields at 400× magnification were selected for quantitative analysis. We calculated the TUNEL staining positive percentage by dividing the TUNEL staining positive cell number with the whole cell number.

Statistical Analysis

Data analysis in the study was performed by the software Graphpad Prism 6.0 version (Graphpad, America). Student's *t*-test was applied for comparison between two groups. A P-value of less than 0.05 on a two-tailed test was considered to be statistically significant in our study.

Results

Preparation and Characterization of DTX-Cur/M Nanomicelles

The synthesis procedure of DTX-Cur/M is illustrated in Figure 1. DTX, Cur and MPEG-PLA copolymers spontaneously assembled to form micelle-like structure. The water-insoluble DTX and Cur were wrapped inside the micelle and administrated into mice through tail vein injection. DTX-Cur/M nanomicelles was supposed to deliver two drugs to the tumor site according to the enhanced permeability and retention effect of tumor vasculature, thus playing an anti-tumor effect.

The molecular dynamic simulation diagram of the interactions between DTX, Cur and MPEG-PLA copolymer was shown in Figures 2 and 3. Results demonstrated that the

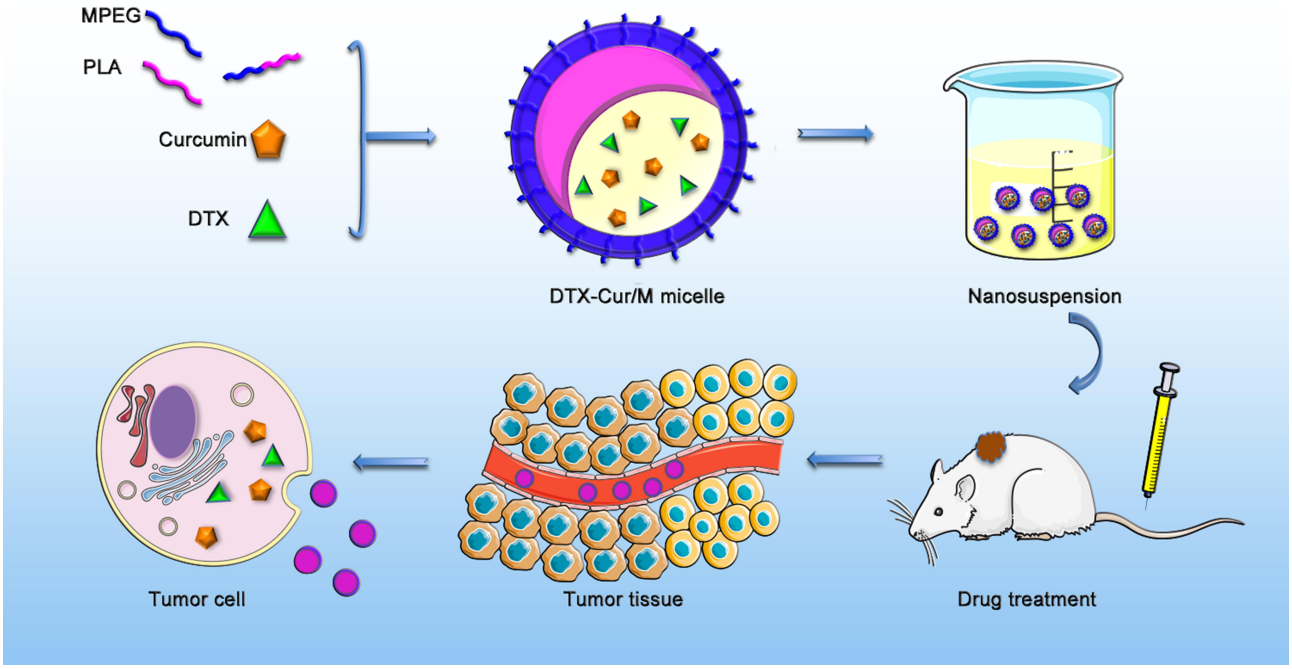

Figure 1 The schematic illustration of synthesis and application of DTX-Cur/M nanomicelle. The DTX-Cur/M micelles were prepared with DTX, Cur and MPEG-PLA polymers by self-assembly method. The drugs were delivered by the micelles after intravenous injection and played anti-tumor effect in vivo.

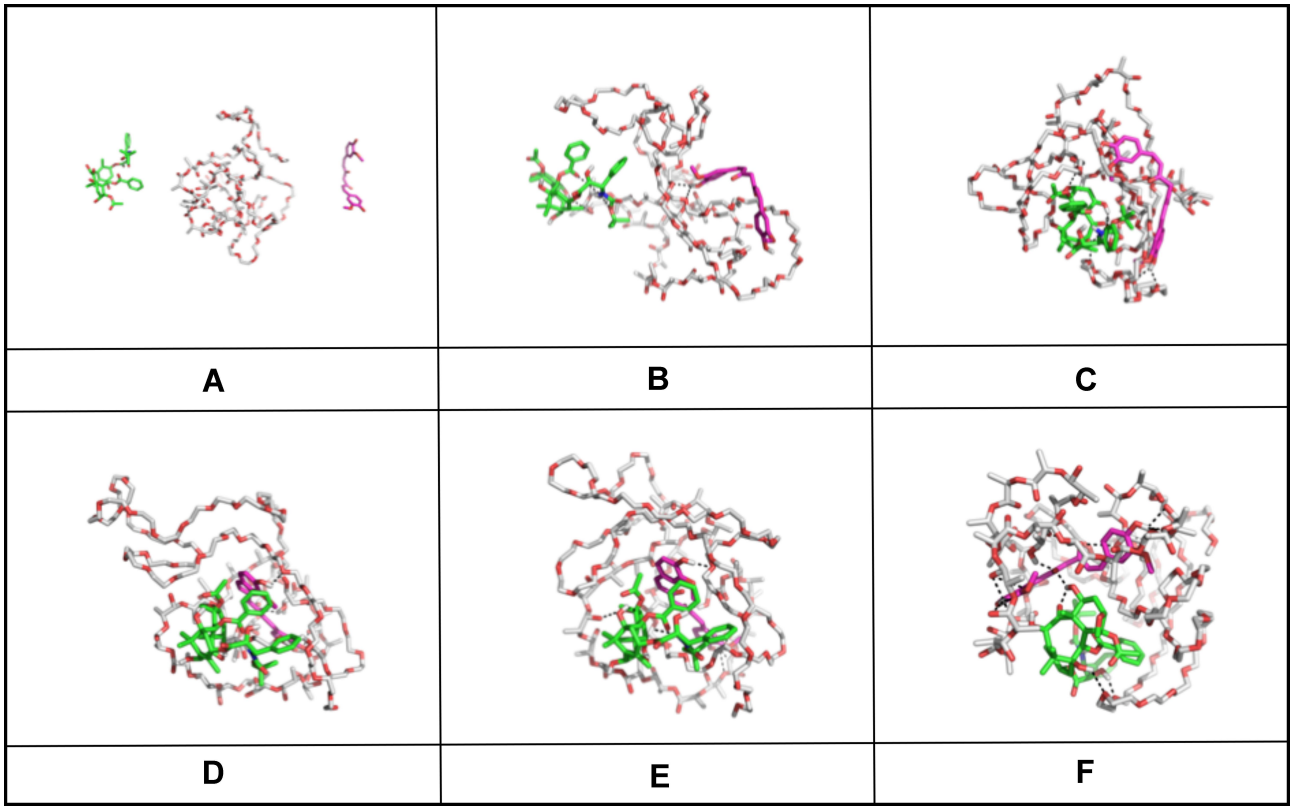

Figure 2 The molecular dynamic simulation diagram of DTX, Cur and MPEG-PLA in aqueous environment. The MPEG-PLA copolymer was depicted by a thin stick. DTX was depicted by a thick stick with green carbon atoms. Cur was depicted by a rosy thick stick. (**A**) Initial structure of DTX, Cur and MPEG-PLA copolymer; (**B**–**F**) Conformations captured at 50ps, 100ps, 200ps, 300ps and 400ps, respectively.

interaction between DTX, Cur and MPEG-PLA copolymer in aqueous environment made them gradually approach each other. DTX and Cur tried to find a suitable place for interaction on the surface of MPEG-PLA copolymer by constantly re-adjusting their position and conformation. In the meantime, MPEG-PLA copolymer continuously adjusted its conformation to provide site for DTX and Cur, thus the interactions between them were strengthened (Figures 2 and 3). The average size and the zeta potential of DTX-Cur /M nanomicelles were 37.63±1.08 nm and −2.00±0.71 mV, respectively (Figure 4A and B). The polydispersity index (PDI) of the particle size was 0.146. Moreover, DTX-Cur /M nanomicelles had a DL of 5% and an EE of 99.2% for DTX, a DL of 5% and an EE of 98.6% for Cur. According to the observation under TEM, DTX-Cur/M nanomicelles showed a spherical morphology (Figure 4C). We further evaluated in vitro drug release of DTX and Cur from DTX-Cur/M in PBS condition. As shown in Figure 4D, the cumulative release of Cur from DTX-Cur/M was 60.07%±3.09 at 120 hrs. The cumulative release of DTX from DTX-Cur/M was 49.57%±2.41 at 120 hrs. The DTX-Cur/M nanomicelles showed sustained drug release behavior.

Cell Cytotoxicity

The cytotoxicity of various concentrations of Cur/M, DTX/M and DTX-Cur/M were investigated by MTT assay. All treatment showed dose-dependent inhibitory effect on A2780 tumor cell viability. According to the results, the cell viability of A2780 cells was decreased with time increase (Figure 5A and B). The IC_{50} of Cur/M, DTX/M and DTX-Cur/M at 48 hrs were 4.42 μg/mL, 0.15 μg/mL and 0.10 μg/mL, respectively (Figure 5B). It was revealed that DTX-Cur/M had stronger tumor cell cytotoxicity than Cur/M or DTX/M in vitro.

Apoptotic Study

Further study was performed to explore if the treatment had an effect on tumor cell apoptosis. According to the flow cytometry results, the Annexin-V positive cells percentage of Cur/M group, DTX/M group and DTX-Cur/M group was 5.62%, 6.59% and 5.06% at the concentration of 0 μg/mL. The Annexin-V positive cells percentage of Cur/M group, DTX/M group and DTX-Cur/M group was 8.79%, 15.44% and 22.92% at the concentration of 0.5 μg/mL (Figure 6). The Annexin-V positive cells percentage of Cur/M group,

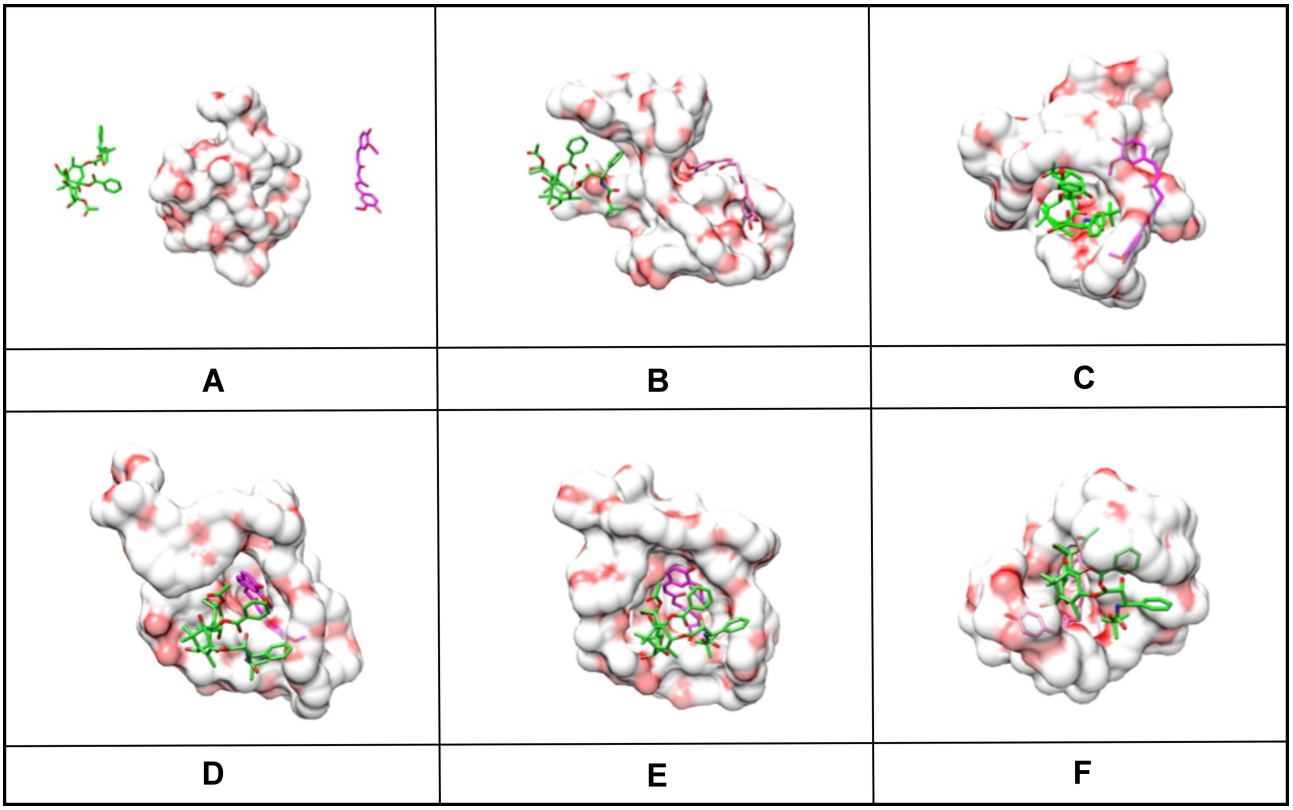

Figure 3 The molecular dynamic simulation diagram of DTX, Cur and MPEG-PLA in aqueous environment. The MPEG-PLA copolymer was depicted by a red and white complex. DTX was depicted by a thick stick with green carbon atoms. Cur was depicted by a rosy thick stick. (**A**) Initial structure of DTX, Cur and MPEG-PLA copolymer; (**B**–**F**) Conformations captured at 50ps, 100ps, 200ps, 300ps and 400ps, respectively.

DTX/M group and DTX-Cur/M group was 10.99%, 16.78% and 23.05% at the concentration of 1 μg/mL (Figure 6). The Annexin-V positive cells percentage of Cur/M group, DTX/M group and DTX-Cur/M group was 9.78%, 24.9% and 29.24% at the concentration of 2 μg/mL (Figure 6). As the increase of drug concentration, there was an increase of Annexin-V staining positive cells. What's more, DTX-Cur/M treated group showed higher apoptosis rate than Cur/M treated group and DTX/M treated group at equivalent concentrations of Cur or DTX, suggesting enhanced anti-tumor efficacy with drug combination.

In vivo Anti-Tumor Activity

With the aim to identify the anti-tumor ability of different drug formulations in vivo, we established a xenograft mice model of human ovarian cancer and gave control, M, Cur/M, DTX/M and DTX-Cur/M treatments to the tumor-bearing mice. There was no significance in mice body weight between control group and other groups, except for DTX-Cur/M group ($P<0.05$), which might be attributed to reduced tumor weight (Figure 7A). The tumor volume of mice in the control group, M group, Cur/M group and DTX/M group increased gradually with time, while that of mice in the DTX-Cur/M group increased slightly. The calculated tumor inhibition rate of M group, Cur/M group, DTX/M group and DTX-Cur/M treatment was 3.02%, 26.12%, 36.31%, 85.96%, respectively (Figure 7B). Consistent with the above results, the mice in Cur/M group, DTX/M group and DTX-Cur/M group all showed a decrease in tumor weight, among which, the DTX-Cur/M group was the most significant (Figure 7C). Representative photographes of subcutaneous tumors from different groups is shown in Figure 7D. These findings demonstrate the anti-tumor efficacy of Cur/M, DTX/M and DTX-Cur/M and also confirm that the therapeutic effect of DTX-Cur/M was the strongest in vivo.

Effect on Proliferation, Angiogenesis and Apoptosis

Further studies were conducted to disclose potential anti-tumor mechanisms of the treatments in the experiment. We evaluated the tumor proliferation status in tumor tissue sections from different treatment groups by Ki67 staining method. High Ki67 index usually indicated active

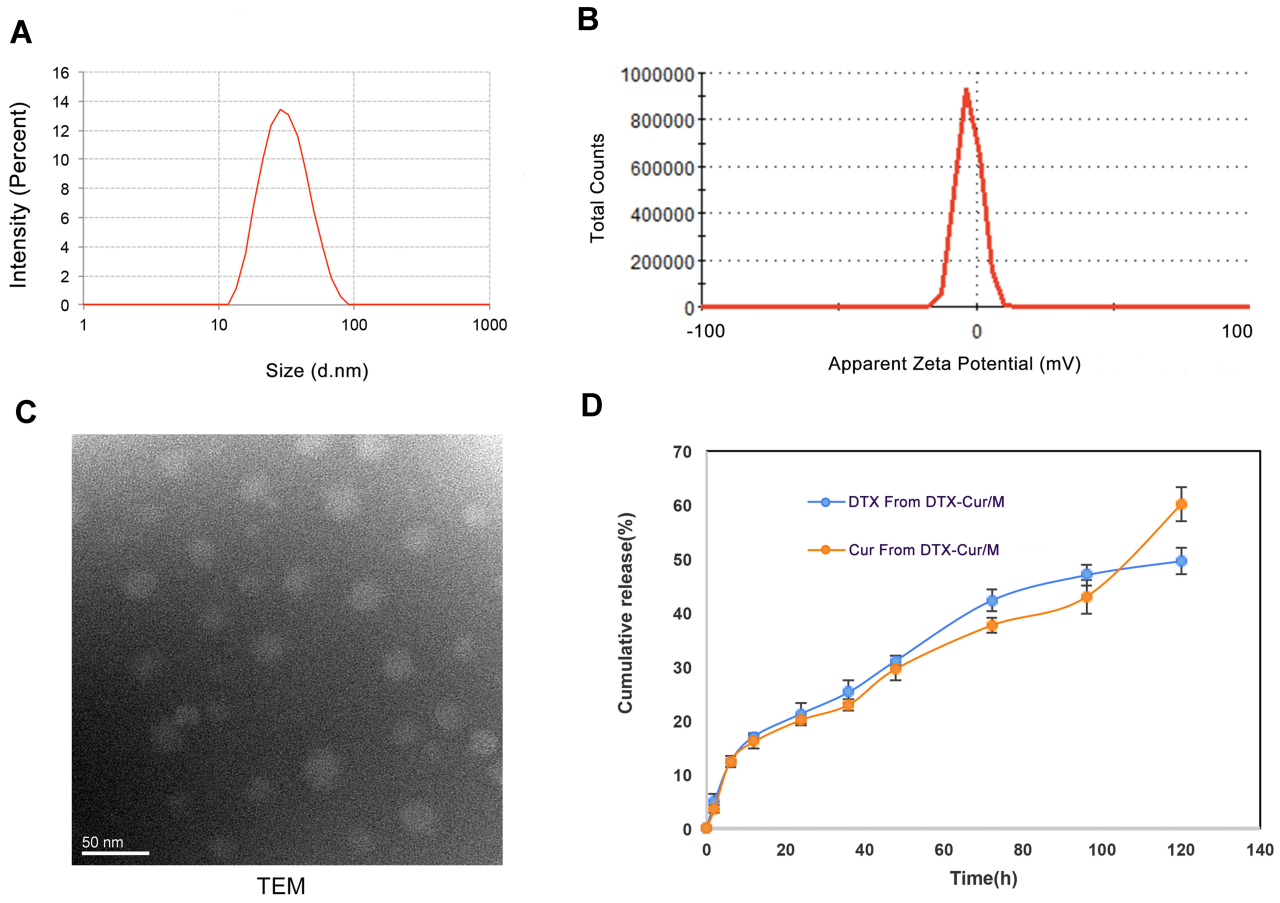

Figure 4 Characterization and drug release of DTX-Cur/M micelles. (**A**) The size distribution of DTX-Cur/M micelles. (**B**) The zeta potential of DTX-Cur/M micelles. (**C**) The morphology under TEM observation. (**D**) The cumulative drug release profile of DTX and Cur from DTX-Cur/M.

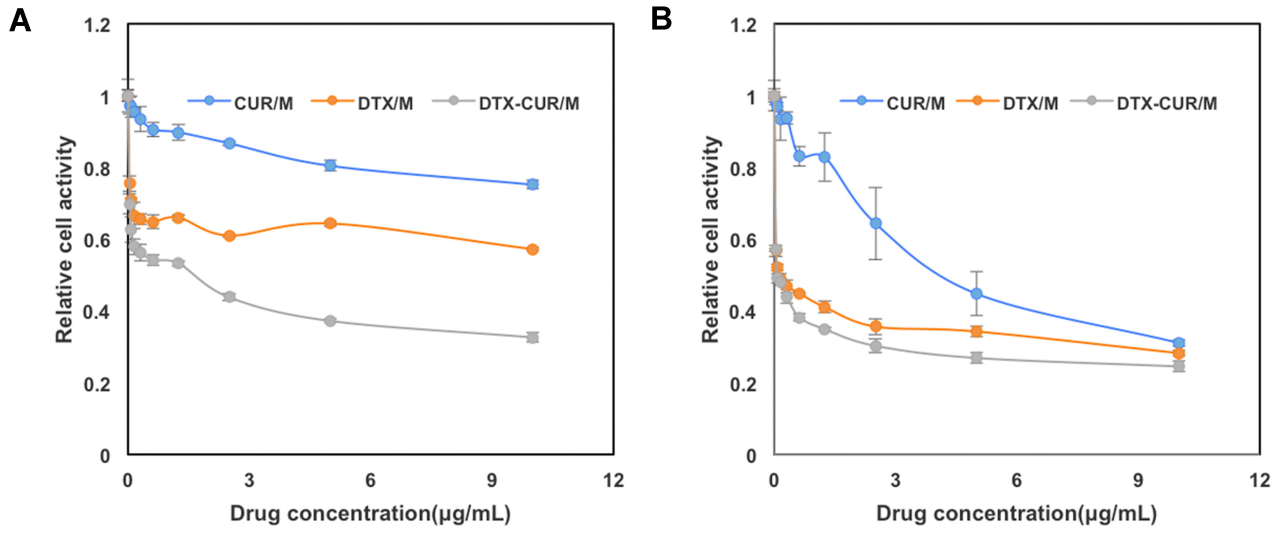

Figure 5 The cytotoxicity of different drug formulations in A2780 cells. (**A**) The cellular viability of A2780 cells from different treatment groups after 24 hrs. (**B**) The cellular viability of A2780 cells from different treatment groups after 48 hrs.

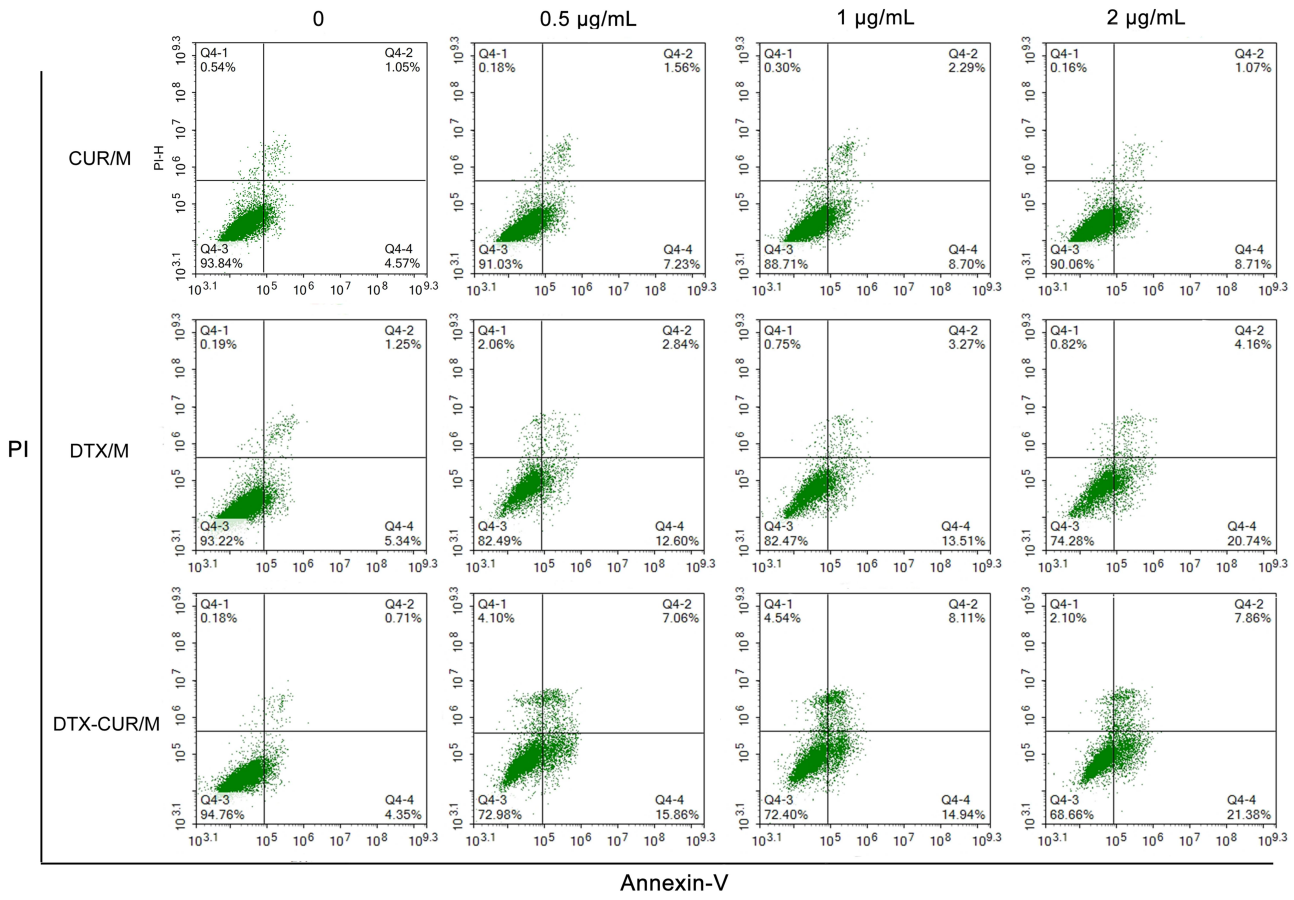

Figure 6 Cell Apoptotic study in A2780 cells. A2780 cells treated with different concentrations of Cur-M, DTX-M and DTX-Cur/M for 48 hrs were labelled by PI/Annexin-V FITC to analyze cell apoptosis.

proliferation status in tumor site, suggesting poor prognosis. Herein, Ki67 index was identified as Ki67 staining positive cells amount divided by total cell amounts. The results showed no obvious changes in Ki67 index between Control group and M group. However, there was a significant decline of Ki67 index after the treatment of Cur/M, DTX/M or DTX-Cur/M formulation, showing the proliferation inhibitory effect of three drug formulations (Figure 8A–F). Besides, DTX-Cur/M group had the minimum Ki67 index among all treatment groups (Figure 8F).

Moreover, we performed the CD31 immunohistochemical staining on tumor sections and estimated tumor angiogenesis activity via counting CD31 positive cells amounts in randomly selected fields. As shown in Figure 9, the number of CD31 positive cells was obviously reduced after Cur/M treatment, DTX/M treatment and DTX-Cur/M treatment. Compared with Cur/M alone or DTX/M alone, DTX-Cur /M showed much stronger ability on suppressing tumor angiogenesis (Figure 9A–F). In addition, the TUNEL assay was conducted to investigate tumor apoptosis. Similar to the results in vitro, the DTX-Cur/M group had the smallest percentage of TUNEL staining positive cells among all treatment groups, suggesting the most powerful capability to promoting apoptosis (Figure 10A–F). In summary, the Cur/M, DTX/M and DTX-Cur/M formulations could play an anti-tumor role through inhibiting tumor proliferation, suppressing tumor angiogenesis and promoting tumor apoptosis. The DTX-Cur/M formulation significantly improved the treatment efficacy of Cur/M and DTX/M formulations.

Discussion

Ovarian cancer is a stubborn gynecological malignancy and often refractory to chemotherapy. The semi-synthetic DTX was considered as an attractive alternative to PTX in ovarian cancer treatment, whose therapeutic effect had been confirmed in clinical trials.[41,42] DTX has the disadvantage of poor water-solubility as PTX, and is usually dissolved in Tween 80 and ethanol for commercial use, leading to hypersensitivity reactions.[43] In the study, our team successfully prepared injectable nanomicelles of

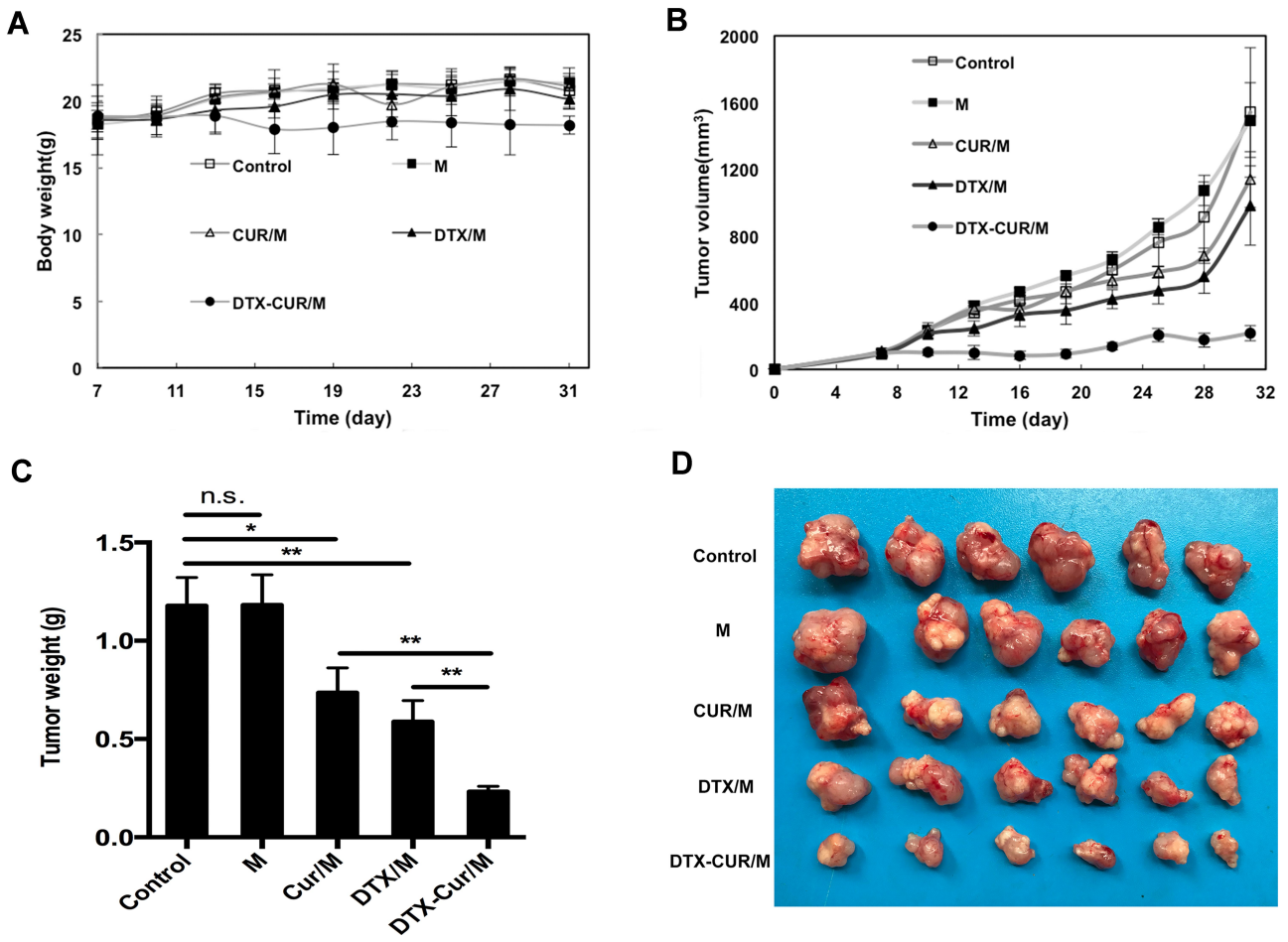

Figure 7 The in vivo anti-tumor evaluation of DTX-Cur/M micelles. (**A**) The curve of mice body weight change. (**B**) Tumor growth curve during the treatment. (**C**) Tumor weight of all treatment groups. (**D**) Photograph of subcutaneous tumors from all treatment groups (*P<0.05, **P<0.01).

DTX-Cur/M with average particle size of 37.63 nm. The drug delivery system could co-deliver DTX and Cur for ovarian cancer therapy to improve the anti-tumor effect and reduce adverse effect.

MPEG-PLA copolymers are biodegradable and stable vehicles for drug delivery, showing benefits in many anti-tumor drug research.[44–47] In this study, the synthesized DTX-Cur/M has high DL and high EE. The drug release experiment found sustained release of DTX and Cur from DTX-Cur/M nanomicelles. The micellar structure was supposed to entrap the poorly water-soluble DTX and Cur in the hydrophobic PLA core region and improve the drug solubility with a PEG shell. After intravenous administration, DTX and Cur would be co-delivered to tumor site due to the enhanced retention and permeability effect of nanoparticle. Thereafter, the DTX-Cur/M possessed unique advantages over traditional DTX and Cur drug combination.

Although the anti-tumor ability of DTX in ovarian cancer has been profoundly demonstrated, the combined drug strategy resulted in more effective anti-tumor activities in the study. Cur, as a preventive and therapeutic drug agent in cancer therapy, is involved in various activities such as cell cycle arrest, apoptosis and angiogenesis.[48] It was found to enhance the efficacy of chemotherapeutic drug when used in combination.[47,49,50] Our study found the DTX-Cur/M treatment significantly inhibited A2780 cell viability. The apoptotic flow cytometry result showed that DTX-Cur/M treatment induced more tumor cell apoptosis than DTX/M monotherapy or Cur/M monotherapy, suggesting a stronger anti-tumor ability. DTX was mainly metabolized by cytochrome CYP3A enzyme, which could be inhibited by Cur, thereby enhancing the anti-tumor performance of DTX. Cur was also effective to inhibit the function of P-glycoprotein (P-gp)-a member of ATP-binding cassette family, which could pump drug extracellular and lead to multi-drug resistance (MDR), thus to

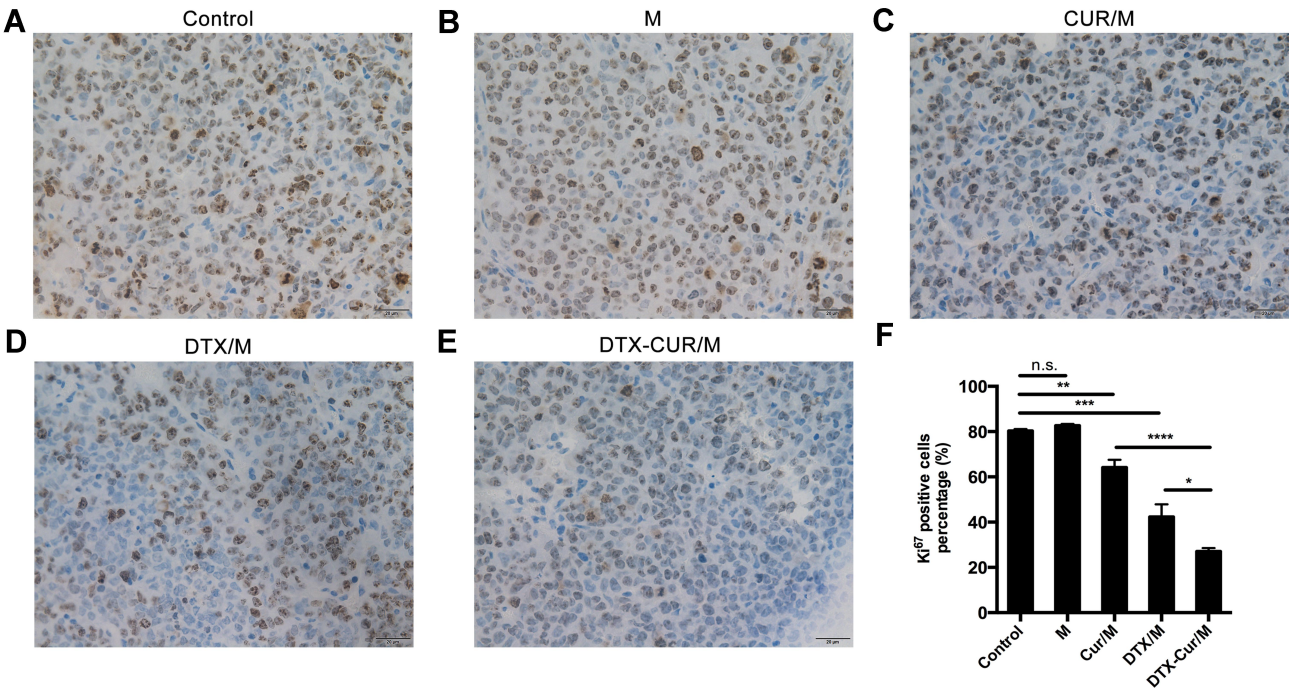

Figure 8 Tumor proliferation assessment with Ki67 staining. Ki67 staining positive cells percentage in (**A**) Control group, (**B**) M group, (**C**) Cur/M group, (**D**) DTX/M group and (**E**) DTX-Cur/M group, (**F**) Statistical Analysis (*P<0.05, **P<0.01, ***P<0.001, ****P<0.0001).

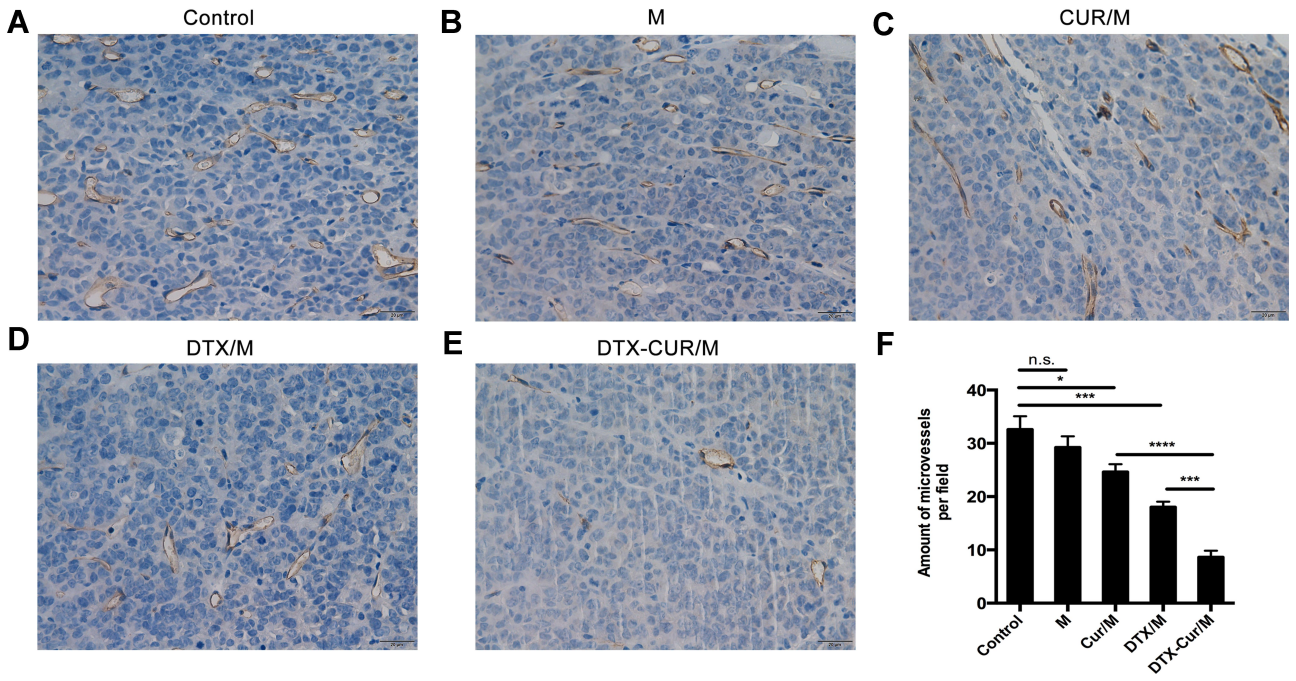

Figure 9 Tumor angiogenesis analysis with CD31 staining. Micro-vessel density in (**A**) Control group, (**B**) M group, (**C**) Cur/M group, (**D**) DTX/M group and (**E**) DTX-Cur /M group, (**F**) Statistical Analysis (*P<0.05, ***P<0.001, ****P<0.0001).

increase the intracellular drug concentration of DTX.[51] In addition, it was reported that Cur was able to counteract the activation of NF-κB signal pathway caused by Taxol.[52] Moreover, Cur could potentiate the anti-tumor capability of DTX with nelfinavir by inducing ER stress in castration resistant prostate cancer cells.[53] Thereupon, the combination of Cur can significantly strengthen the anti-tumor activity of DTX. Although some research has reported the application of DTX and Cur in cancer treatment, our study successfully encapsulated dual drug agents in the

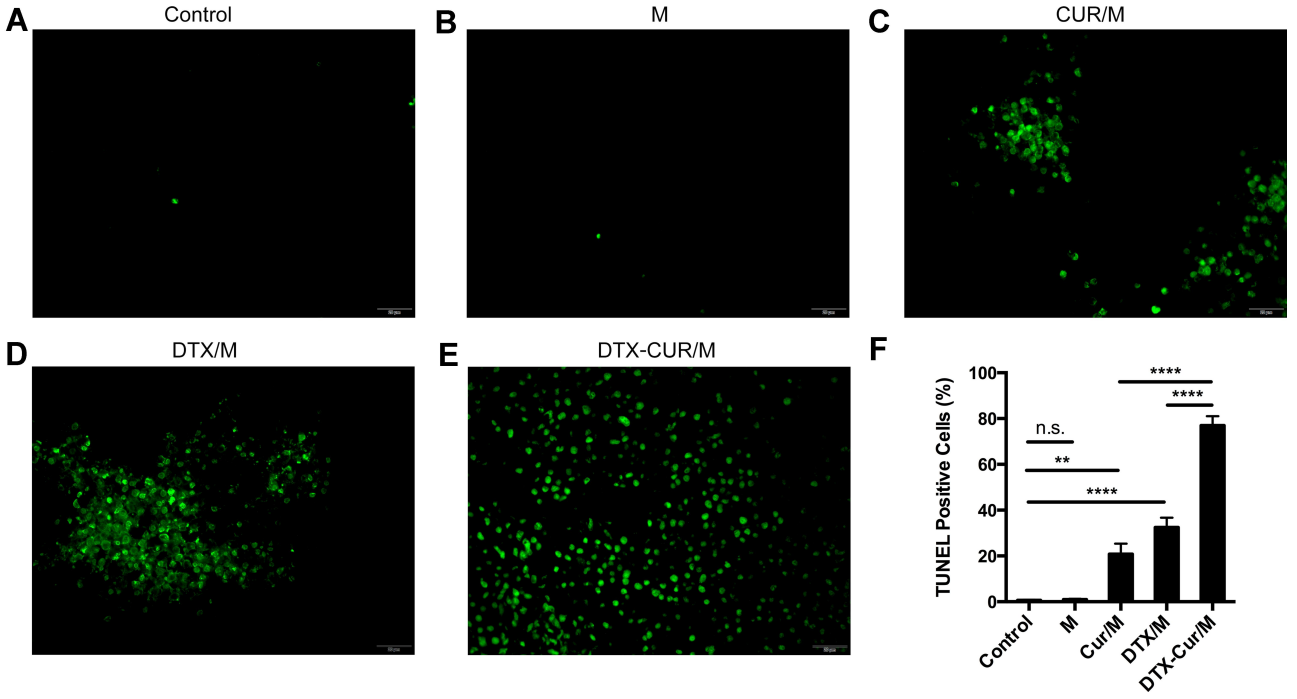

Figure 10 Tumor apoptosis assay with TUNEL staining. TUNEL staining positive cells percentage in (**A**) Control group, (**B**) M group, (**C**) Cur/M group, (**D**) DTX/M group and (**E**) DTX-Cur/M group, (**F**) Statistical Analysis (**P<0.01, ****P<0.0001).

MPEG-PLA copolymer based drug delivery system, thus achieving direct co-delivery to tumor site for ovarian cancer therapy.

The efficacy assessment in mice ovarian cancer model indicated that tumor growth was significantly suppressed by the treatment of Cur/M nanomicelles, DTX/M nanomicelles and DTX-Cur/M nanomicelles. The tumor volume and tumor weight of DTX-Cur/M group were the minimum among all treatment groups, suggesting DTX-Cur/M nanomicelles had the most powerful anti-tumor capability. In the mechanism, we further demonstrated that DTX-Cur /M nanomicelles were able to inhibit tumor proliferation, suppress tumor angiogenesis and promote tumor apoptosis in vivo. Besides, no significant adverse events were observed after combined use of DTX and Cur, indicating that DTX-Cur/M is a beneficial agent with good safety and low toxicity. Taken together, DTX-Cur/M nanomicelles may exhibit the benefits of improved bioavailability, good biodegradability and integrated therapeutic effect of dual drugs, making it a promising drug formulation for ovarian cancer therapy.

Conclusions

In the study, a core-shell structure of MPEG-PLA copolymers was successfully synthesized to encapsulate and co-deliver DTX and Cur for the treatment of ovarian cancer. The DTX-Cur/M nanomicelles had a homogeneous particle size and sustained drug release behavior. The DTX-Cur /M nanomicelles were able to inhibit ovarian cancer cells viability and promote cells apoptosis in vitro. In vivo drug evaluation showed significantly enhanced anti-tumor effect in terms of suppressing tumor cell proliferation, attenuating tumor angiogenesis and promoting tumor cell apoptosis. In summary, the DTX-Cur/M nanomicelle is a biodegradable, sustainable and powerful anti-tumor drug formulation with great potential in ovarian cancer therapy.

Funding

This work was supported by the Ministry of Science and Technology of the People's Republic of China (No. 2018ZX09201018), China Postdoctoral Science Foundation (No. 2019M663515) and the Key R&D Projects of the Science and Technology Department of Sichuan Province (No. 2019YFS0340, No. 2020YFS0213).

Disclosure

The authors report no conflicts of interest in this work.

References

1. Odunsi K. Immunotherapy in ovarian cancer. *Ann Oncol*. 2017;28 (suppl8):viii1–viii7. doi:10.1093/annonc/mdx444

2. Rooth C. Ovarian cancer: risk factors, treatment and management. *Br J Nurs*. 2013;22(17):S23–30. doi:10.12968/bjon.2013.22.Sup17.S23
3. Stuart GC. First-line treatment regimens and the role of consolidation therapy in advanced ovarian cancer. *Gynecol Oncol*. 2003;90(3 Pt 2):S8–15. doi:10.1016/S0090-8258(03)00472-4
4. Cannistra SA. Cancer of the ovary. *N Engl J Med*. 2004;351(24):2519–2529. doi:10.1056/NEJMra041842
5. Bookman MA, Brady MF, McGuire WP, et al. Evaluation of new platinum-based treatment regimens in advanced-stage ovarian cancer: a phase III trial of the gynecologic cancer intergroup. *J Clin Oncol*. 2009;27(9):1419–1425. doi:10.1200/JCO.2008.19.1684
6. Jayson GC, Kohn EC, Kitchener HC, Ledermann JA. Ovarian cancer. *Lancet*. 2014;384(9951):1376–1388. doi:10.1016/S0140-6736(13)62146-7
7. Ray-Coquard I, Pautier P, Pignata S, et al. Olaparib plus bevacizumab as first-line maintenance in ovarian cancer. *N Engl J Med*. 2019;381(25):2416–2428. doi:10.1056/NEJMoa1911361
8. Pujade-Lauraine E, Ledermann JA, Selle F, et al. Olaparib tablets as maintenance therapy in patients with platinum-sensitive, relapsed ovarian cancer and a BRCA1/2 mutation (SOLO2/ENGOT-Ov21): a double-blind, randomised, placebo-controlled, phase 3 trial. *Lancet Oncol*. 2017;18(9):1274–1284.
9. Prat J. FIGO's staging classification for cancer of the ovary, fallopian tube, and peritoneum: abridged republication. *J Gynecol Oncol*. 2015;26(2):87–89. doi:10.3802/jgo.2015.26.2.87
10. Montero A, Fossella F, Hortobagyi G, Valero V. Docetaxel for treatment of solid tumours: a systematic review of clinical data. *Lancet Oncol*. 2005;6(4):229–239. doi:10.1016/S1470-2045(05)70094-2
11. Cortes JE, Pazdur R. Docetaxel. *J Clin Oncol*. 1995;13(10):2643–2655. doi:10.1200/JCO.1995.13.10.2643
12. Tan Q, Liu X, Fu X, et al. Current development in nanoformulations of docetaxel. *Expert Opin Drug Deliv*. 2012;9(8):975–990. doi:10.1517/17425247.2012.696606
13. Kelland LR, Abel G. Comparative in vitro cytotoxicity of taxol and Taxotere against cisplatin-sensitive and -resistant human ovarian carcinoma cell lines. *Cancer Chemother Pharmacol*. 1992;30(6):444–450. doi:10.1007/BF00685595
14. Haldar S, Basu A, Croce CM. Bcl2 is the guardian of microtubule integrity. *Cancer Res*. 1997;57(2):229–233.
15. Vasey PA, Jayson G, Gordon A, et al. Phase III randomized trial of docetaxel-carboplatin versus paclitaxel-carboplatin as first-line chemotherapy for ovarian carcinoma. *J Natl Cancer Inst*. 2004;96(22):1682–1691. doi:10.1093/jnci/djh323
16. Miles DW, Chan A, Dirix L, et al. Phase III study of bevacizumab plus docetaxel compared with placebo plus docetaxel for the first-line treatment of human epidermal growth factor receptor 2-negative metastatic breast cancer. *J Clin Oncol*. 2010;28(20):3239–3247. doi:10.1200/JCO.2008.21.6457
17. Argiris A, Ghebremichael M, Gilbert J, et al. Phase III randomized, placebo-controlled trial of docetaxel with or without gefitinib in recurrent or metastatic head and neck cancer: an eastern cooperative oncology group trial. *J Clin Oncol*. 2013;31(11):1405–1414. doi:10.1200/JCO.2012.45.4272
18. Baxi SS, Sher DJ, Pfister DG. Value considerations in the treatment of head and neck cancer: radiation, chemotherapy, and supportive care. *Am Soc Clin Oncol Educ Book*. 2014;34:e296–303. doi:10.14694/EdBook_AM.2014.34.e296
19. Ford HE, Marshall A, Bridgewater JA, et al. Docetaxel versus active symptom control for refractory oesophagogastric adenocarcinoma (COUGAR-02): an open-label, phase 3 randomised controlled trial. *Lancet Oncol*. 2014;15(1):78–86. doi:10.1016/S1470-2045(13)70549-7
20. Abotaleb M, Kubatka P, Caprnda M, et al. Chemotherapeutic agents for the treatment of metastatic breast cancer: an update. *Biomed Pharmacother*. 2018;101:458–477. doi:10.1016/j.biopha.2018.02.108
21. Reck M, Garassino MC, Imbimbo M, et al. Antiangiogenic therapy for patients with aggressive or refractory advanced non-small cell lung cancer in the second-line setting. *Lung Cancer*. 2018;120:62–69. doi:10.1016/j.lungcan.2018.03.025
22. Halabi S, Dutta S, Tangen CM, et al. Overall survival of black and white men with metastatic castration-resistant prostate cancer treated with docetaxel. *J Clin Oncol*. 2019;37(5):403–410. doi:10.1200/JCO.18.01279
23. Zahedi P, De Souza R, Huynh L, et al. Combination drug delivery strategy for the treatment of multidrug resistant ovarian cancer. *Mol Pharm*. 2011;8(1):260–269. doi:10.1021/mp100323z
24. Zhang W, Huang Z, Pu X, et al. Fabrication of doxorubicin and chlorotoxin-linked Eu-Gd2O3 nanorods with dual-model imaging and targeted therapy of brain tumor. *Chinese Chem Lett*. 2020;31(1):285–291. doi:10.1016/j.cclet.2019.04.018
25. Yang T, Ming X, Jie L, et al. Ultrasound-triggered nanodroplets for targeted co-delivery of sorafenib/doxorubicin for hepatocellular carcinoma therapy. *J Biomed Nanotechnol*. 2019;15(9):1881–1896. doi:10.1166/jbn.2019.2823
26. Goel A, Kunnumakkara A, Aggarwal BB. Curcumin as "Curecumin": from kitchen to clinic. *Biochem Pharmacol*. 2008;75(4):787–809. doi:10.1016/j.bcp.2007.08.016
27. Aggarwal BB, Harikumar KB. Potential therapeutic effects of curcumin, the anti-inflammatory agent, against neurodegenerative, cardiovascular, pulmonary, metabolic, autoimmune and neoplastic diseases. *Int J Biochem Cell Biol*. 2009;41(1):40–59. doi:10.1016/j.biocel.2008.06.010
28. Anand P, Sundaram C, Jhurani S, Kunnumakkara A, Aggarwal BB. Curcumin and cancer: an "old-age" disease with an "age-old" solution. *Cancer Lett*. 2008;267(1):133–164. doi:10.1016/j.canlet.2008.03.025
29. Zhang T, Chen Y, Ge Y, Hu Y, Li M, Jin Y. Inhalation treatment of primary lung cancer using liposomal curcumin dry powder inhalers. *Acta Pharm Sin B*. 2018;8(3):440–448. doi:10.1016/j.apsb.2018.03.004
30. Yang Z, Peng Y, Qiu L. pH-Responsive supramolecular micelle based on host-guest interaction of poly(β-amino ester) derivatives and adamantyl-terminated poly(ethylene glycol) for cancer inhibition. *Chinese Chem Lett*. 2018;29(12):1839–1844. doi:10.1016/j.cclet.2018.11.009
31. van Herwaarden AE, Wagenaar E, van der Kruijssen CM, et al. Knockout of cytochrome P450 3A yields new mouse models for understanding xenobiotic metabolism. *J Clin Invest*. 2007;117(11):3583–3592. doi:10.1172/JCI33435
32. Woo J, Lee CH, Shim CK, Hwang S. Enhanced oral bioavailability of paclitaxel by coadministration of the P-glycoprotein inhibitor KR30031. *Pharm Res*. 2003;20(1):24–30. doi:10.1023/A:1022286422439
33. Valentine SP, Le Nedelec MJ, Menzies AR, et al. Curcumin modulates drug metabolizing enzymes in the female Swiss Webster mouse. *Life Sci*. 2006;78(20):2391–2398. doi:10.1016/j.lfs.2005.09.017
34. Yan Y, Kim D, Sung JH, Yong CS, Choi HG. Enhanced oral bioavailability of docetaxel in rats by four consecutive days of pre-treatment with curcumin. *Int J Pharm*. 2010;399(1–2):116–120. doi:10.1016/j.ijpharm.2010.08.015
35. Anand P, Kunnumakkara AB, Newman RA, et al. Bioavailability of curcumin: problems and promises. *Mol Pharm*. 2007;4(6):807–818. doi:10.1021/mp700113r
36. Liu X, Gao X, Zheng S, et al. Modified nanoparticle mediated IL-12 immunogene therapy for colon cancer. *Nanomedicine*. 2017;13(6):1993–2004. doi:10.1016/j.nano.2017.04.006
37. Halgren TA. Merck molecular force field.1. Basis, form, scope, parameterization, and performance of MMFF94. *J Comput Chem*. 1996;17(5–6):490–519.
38. Dewar MJS, Zoebisch EG, Healy EF, Stewart JJP. The development and use of quantum-mechanical molecular-models.76. AM1 - a new general-purpose quantum-mechanical molecular-model. *J Am Chem Soc*. 1985;107(13):3902–3909. doi:10.1021/ja00299a024

39. Gong C, Xie Y, Wu Q, et al. Improving anti-tumor activity with polymeric micelles entrapping paclitaxel in pulmonary carcinoma. *Nanoscale*. 2012;4(19):6004–6017. doi:10.1039/c2nr31517c
40. Hu Y, Wu C, Zhu C, et al. Enhanced uptake and improved anti-tumor efficacy of doxorubicin loaded fibrin gel with liposomal apatinib in colorectal cancer. *Int J Pharm*. 2018;552(1–2):319–327. doi:10.1016/j.ijpharm.2018.10.013
41. Aravantinos G, Bafaloukos D, Fountzilas G, et al. Phase II study of docetaxel-vinorelbine in platinum-resistant, paclitaxel-pretreated ovarian cancer. *Ann Oncol*. 2003;14(7):1094–1099. doi:10.1093/annonc/mdg292
42. Wenham RM, Lapolla J, Lin H, et al. A phase II trial of docetaxel and bevacizumab in recurrent ovarian cancer within 12 months of prior platinum-based chemotherapy. *Gynecol Oncol*. 2013;130(1):19–24. doi:10.1016/j.ygyno.2013.04.049
43. Gelderblom H, Verweij J, Nooter K, Sparreboom A. Cremophor EL: the drawbacks and advantages of vehicle selection for drug formulation. *Eur J Cancer*. 2001;37(13):1590–1598. doi:10.1016/S0959-8049(01)00171-X
44. He Y, Wu C, Duan J, Miao J, Ren H, Liu J. Anti-glioma effect with targeting therapy using folate modified nano-micelles delivery curcumin. *J Biomed Nanotechnol*. 2020;16(1):1–13. doi:10.1166/jbn.2020.2878
45. Mu CF, Balakrishnan P, Cui F, et al. The effects of mixed MPEG-PLA/Pluronic copolymer micelles on the bioavailability and multidrug resistance of docetaxel. *Biomaterials*. 2010;31(8):2371–2379. doi:10.1016/j.biomaterials.2009.11.102
46. Dong Y, Feng SS. Methoxy poly(ethylene glycol)-poly(lactide) (MPEG-PLA) nanoparticles for controlled delivery of anticancer drugs. *Biomaterials*. 2004;25(14):2843–2849. doi:10.1016/j.biomaterials.2003.09.055
47. Zheng X, Kan B, Gou M, et al. Preparation of MPEG-PLA nanoparticle for honokiol delivery in vitro. *Int J Pharm*. 2010;386(1–2):262–267. doi:10.1016/j.ijpharm.2009.11.014
48. Hu Y, He Y, Ji J, Zheng S, Cheng Y. Tumor targeted curcumin delivery by folate-modified MPEG-PCL self-assembly micelles for colorectal cancer therapy. *Int J Nanomed*. 2020;15:1239–1252. doi:10.2147/IJN.S232777
49. Cruz-Correa M, Shoskes DA, Sanchez P, et al. Combination treatment with curcumin and quercetin of adenomas in familial adenomatous polyposis. *Clin Gastroenterol Hepatol*. 2006;4(8):1035–1038. doi:10.1016/j.cgh.2006.03.020
50. Narayanan NK, Nargi D, Randolph C, Narayanan BA. Liposome encapsulation of curcumin and resveratrol in combination reduces prostate cancer incidence in PTEN knockout mice. *Int J Cancer*. 2009;125(1):1–8.
51. Chearwae W, Anuchapreeda S, Nandigama K, et al. Biochemical mechanism of modulation of human P-glycoprotein (ABCB1) by curcumin I, II, and III purified from turmeric powder. *Biochem Pharmacol*. 2004;68(10):2043–2052. doi:10.1016/j.bcp.2004.07.009
52. Bava SV, Puliyappadamba VT, Deepti A, Nair A, Karunagaran D, Anto RJ. Sensitization of taxol-induced apoptosis by curcumin involves down-regulation of nuclear factor- B and the serine/threonine kinase Akt and is independent of tubulin polymerization (vol 280, pg 6301, 2005). *J Biol Chem*. 2018;293(31):12283. doi:10.1074/jbc.AAC118.004745
53. Mathur A, Abd Elmageed ZY, Liu X, et al. Subverting ER-stress towards apoptosis by nelfinavir and curcumin coexposure augments docetaxel efficacy in castration resistant prostate cancer cells. *PLoS One*. 2014;9(8):e103109. doi:10.1371/journal.pone.0103109